Ultrasonic-assisted DES extraction optimization, characterization, antioxidant and *in silico* study of polysaccharides from *Angelica dahurica* Radix

Qian Li [*], Ting Wang, Chenyue Wang, Xiaoqin Ding

College of Agronomy, State Key Laboratory of Aridland Crop Science, Gansu Agricultural University, Lanzhou 730070, China

ARTICLE INFO

ABSTRACT

In this study, polysaccharides from *Angelica dahurica* Radix (ADR) were extracted by using ultrasonic-assisted deep eutectic solvent (DES) extraction method. The DES consist of choline chloride (HBA, hydrogen bonding acceptor) and 1, 4-butanediol (HBD, hydrogen bonding donor) with the molar ratio of 1:3 was proved as the best system for polysaccharides extraction. A Box-Behnken design with three factors and three levels was utilized to optimize ultrasonic power, extraction time and temperature for increased polysaccharides yield. The optimal extraction parameters were determined as follows: DES water content of 20 %, liquid–solid ratio of 10:1 mL/g, ultrasonic time of 21 min, temperature at 60 °C, and ultrasonic power of 435 W. These conditions yielded an extraction rate nearly matching the theoretical predicted value of the response surface model, surpassing the traditional hot water extraction method by 1.33 times and requiring less time. The antioxidant polysaccharides was assessed using DPPH, ABTS and Hydroxyl methods, which indicated that ADRP extracted by ultrasound assisted DES had excellent antioxidant capacity and showed a dose–response relationship with drug concentration. Structural analysis identified ADR polysaccharides as a heteropolysaccharide rich in sugar aldonic acids—namely, fucose, rhamnose, arabinose, galactose and glucose—with molar ratios of 0.47:1.99:17.61:64.76:15.17. The polysaccharides' number-average molecular weight was determined to be 97.422 kDa, with a weight-average molecular weight of 245.678 kDa. Network pharmacology and molecular docking analysis suggest that the monosaccharides Rha and Ara could potentially interact with the proteins GSR and GSTA1, respectively, indicating that ADRP had good antioxidant potential and could be applied in multiple fields with promising development prospects in the future.

1. Introduction

Angelica dahurica Radix (ADR) is a renowned Chinese herbal medicine and edible plant with a history of over a thousand years in China. Traditionally utilized for treating conditions such as colds, headaches, asthma, rhinitis, hypertension, vitiligo and psoriasis (Wang et al., 2017), pharmacological studies have highlighted its antioxidant, antibacteria, anti-tumor, and analgesic properties (Wang et al., 2023a). ADR's main active components encompass coumarins, volatile oils, polysaccharides, and trace elements (Commission National Pharmacopoeia, 2020). The coumarin compounds have been extensively studied, while research on polysaccharides remains limited despite their antioxidant effects and diverse biological activities.

Numerous methods for extracting polysaccharides have been documented. The hot water extraction is the conventional and straightforward method for polysaccharides extraction, it necessitates high temperatures and prolonged extraction periods (Wang et al., 2023b). Ultrasonic extraction as a modern method is extensively employed for extracting polysaccharides from various plant sources due to its ability to enhance mass transfer, disrupt cells, and augment osmosis and capillarity (Zhang et al., 2023).

Deep eutectic solvent (DES) has emerged as a promising alternative to traditional organic solvents, owing to its eco-friendly, non-toxic, biodegradable, and recyclable properties. DES exhibits a strong capability to dissolve a wide range of bioactive compounds such as polysaccharides and proteins, attributed to the robust hydrogen bonding within the solvent structure (Sun et al., 2021). The integration of DES with ultrasonic extraction has garnered significant interest due to its

---

* Corresponding author.
  E-mail address: liqian1984@gsau.edu.cn (Q. Li).

Table 1
Types of DES prepared in this study.

NO.	Hydrogen bond acceptors (HBAs)	Hydrogen bond donors (HBDs)	Molar ration (HBA/HBD)
1	Choline chloride	lactic acid	1:1
2	Choline chloride	lactic acid	1:2
3	Choline chloride	lactic acid	1:3
4	Choline chloride	glycerin	1:1
5	Choline chloride	glycerin	1:2
6	Choline chloride	glycerin	1:3
7	Choline chloride	urea	1:1
8	Choline chloride	urea	1:2
9	Choline chloride	urea	1:3
10	Choline chloride	1,4-butanediol	1:1
11	Choline chloride	1,4-butanediol	1:2
12	Choline chloride	1,4-butanediol	1:3

capacity to enhance extraction efficiency, accelerated the process, and simplified operation.

The experiment designed by the Box-Behnken design (BBD) combined with Response Surface Methodology (RSM) utilizes low, medium, and high levels encoded as − 1, 0, and + 1, enabling a minimization of the number of experiments. Compared to other approaches, this method offers greater efficiency in arranging and elucidating experiments (Chen et al., 2018). In this research, polysaccharides were extracted from ADR by using ultrasonic-assisted deep eutectic solvent extraction. The optimization of ADR polysaccharides extraction parameters was based on the BBD-RSM design.

Polysaccharides have been confirmed by researchers to have antioxidant activity, and their antioxidant potential is typically evaluated through reactions and mechanisms such as free radical scavenging, chain initiation, reduction, and transition metal ions. DPPH, as a stable radical, reacted with an antioxidant molecule with an obvious color change from violet to colorless, providing a rapid and convenient method for antioxidation evaluation (Xie et al., 2015; Wang et al., 2013). ABTS is also based on the elimination of free radicals and is a common method for evaluating antioxidant capacity (Mareček et al., 2017). As an oxygen radical, the hydroxyl radical can initiate free radical chain reactions by attacking almost all biological molecules in the human body, such as lipids, nucleic acids, fatty acids, and carbohydrates (Sun et al., 2015).

ADR, as a traditional herbal remedy, holds extensive applications in the pharmaceutical, food, and cosmetics sectors. The implementation of efficient and eco-friendly extraction methods for ADRP could contribute to the reduction of energy consumption and pollutant emissions during production processes, aligning with the principles of sustainable development. Moreover, investigating the antioxidant properties of ADRP could play a vital role in the prevention and treatment of diseases associated with oxidative stress, laying a solid scientific foundation for the formulation of novel antioxidants to enhance public health. In this study, *Angelica dahurica* Radix polysaccharides (ADRP) were extracted using the ultrasonic-assisted DES extraction method. The chemical structure of ADRP was characterized by employing FT-IR and chromatography. The antioxidant activity of ADRP was investigated in vitro, and the mechanisms of the polysaccharides fractions were explored using network pharmacology and molecular docking techniques.

2. Materials and methods

2.1. Materials

Angelica dahurica Radix was bought from Qingshan Sulfur-free Food Store in Suining city, Sichuan Province China (105°42′15.412″E, 30°45′30.377″N) in May 2023, which was identified as *Angelica dahurica* (Fisch.ex Hoffm.) Benth.et Hook.f.var.formosana (Boiss.) Shan et Yuan by Professor Yuan Chen, Gansu Agricultural University. A proper amount of the herbs was taken and baked for 12 h in the oven at 60℃.

After being crushed and sifted through 40 mesh, the crude powder of ADR was prepared.

All chemicals used for the preparation of DES and for the determination were purchased from companies in several Chinese cities (supporting information).

2.2. Preparation of DESs

It is crucial to carefully select the appropriate DES type for the extraction of the target compound from the sample. In this study, 12 types of DES systems (Table 1) were prepared by using a simple heating method that requires minimal equipment. The detailed experimental process was elaborated in supporting information.

2.3. Extraction of ADRP by DES

Approximately 1.00 g of sieved ADR powder was used to extract ADRP. A pre-prepared DES was added using a liquid–solid ratio of 20:1 mL/g. The ultrasonic extraction conditions included a power setting of 300 W and frequency of 50 Hz, with an ultrasonic duration of 45 min at a temperature of 60 °C for the extraction of polysaccharides. The extract underwent concentration through a rotary evaporator. Following this, the concentrated solution was diluted with anhydrous ethanol at a volume ratio of 1:4 and refrigerated at 4 °C overnight to induce precipitation. Subsequent centrifugation and drying processes yielded the crude polysaccharides product.

2.4. Traditional extraction method comparison

To contrast ultrasound-assisted extraction with hot water extraction, polysaccharides were extracted using hot water in this study. The procedure involved extracting 5.00 g of pretreated sample powder with 150 mL of boiling water for 2 h. After three rounds of extraction, the resultant extracts were combined and subjected to alcohol precipitation to isolate the crude polysaccharides.

2.5. Optimization of the extraction process

The impact of single factor on the yield of ADRP were investigated first. Further, BBD response test with three factors and three levels was utilized to optimize ultrasonic power, extraction time, and temperature for increased polysaccharides yield, and the details are given in the supporting information.

2.6. Structural characterization

The functional groups, molecular weight distribution and monosaccharide composition of ADRP were characterized by Fourier infrared spectroscopy (FT-IR) (Shashidhar et al. 2015), gel chromatography and anion exchange chromatography, respectively. The detailed processes are given in the supporting information.

2.7. Antioxidant activity test in vitro

The DPPH, ABTS and hydroxyl radical scavenging method were used to analyze the samples' antioxidant properties in vitro. Extracts from two methods, traditional hot water and DES ultrasonic-assisted extraction, were compared. Each sample was prepared at maximum extraction concentration, and an ascorbic acid (VC) solution served as a control. The detailed processes are given in the supporting information.

2.8. Network pharmacology and molecular docking analysis

The target proteins for five different sugars of ADRP were analyzed by Network pharmacology methods. Further, how sugars of ADRP interact with proteins was carried out by Molecular docking methods.
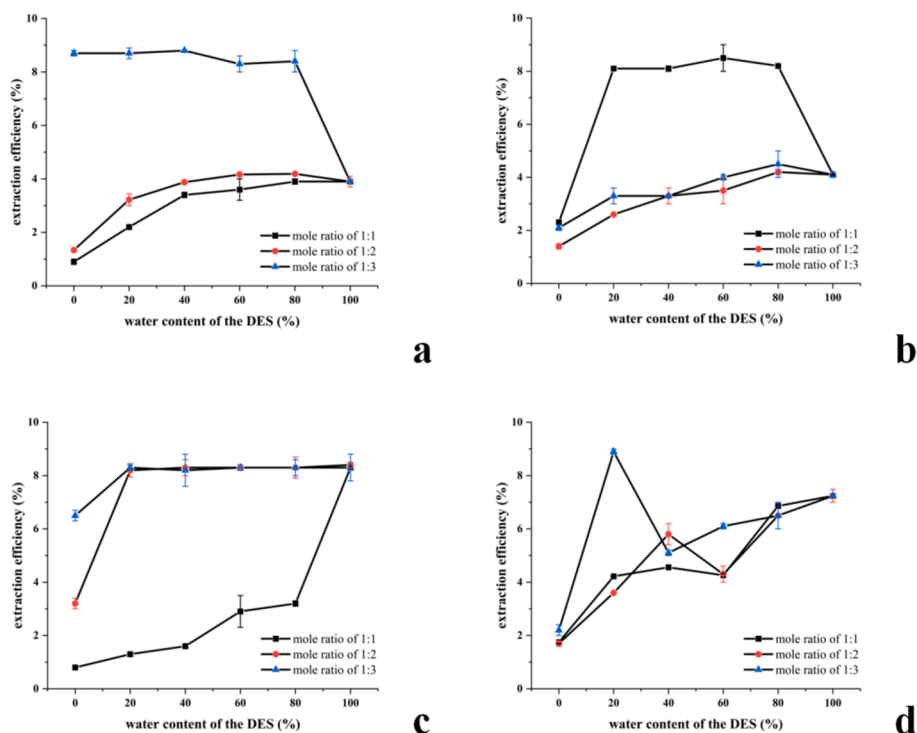
Fig. 1. The results of DES system screening. Extraction rates of polysaccharides with different mole ratios in choline chloride-lactic acid system (a), choline chlorine-glycerol system (b), choline chloride-urea system(c) and choline chloride 1, 4-butanediol system (d).

3. Results and Discussion

3.1. Establishment of glucose standard curve

A glucose standard curve was established by using a UV spectrophotometer (Tomas et al., 2018). The regression equation, $Y = 0.0095x + 0.1647$, depicted in Fig.S1 (supporting information), demonstrates a strong linear relationship within the range of 200 μg/mL to 1000 μg/mL.

3.2. Screening of DES solvent systems

According to the results depicted in Fig. 1, among the four distinct DES systems investigated, the choline chloride-1,4-butanediol system exhibited remarkable extraction efficacy. The maximum extraction rate of ADRP was achieved when the mole ratio was 1:3 and the water content of the DES system was 20 %. This enhancement can be attributed to the abundant hydroxyl groups present in the alcohols within the DES system, which intensify the interaction forces with polysaccharides (Sun et al., 2021), thereby enhancing the extraction efficiency of ADRP. Moreover, at a moisture content of 20 %, the solution's fluidity increases, facilitating more efficient dissolution of the polysaccharides and resulting in a higher extraction rate. Consequently, the most optimal DES system identified for ADRP extraction in this study was 1, 4-butanediol as the HBD. The molar ratio of HBA: HBD was 1:3, with a water content of 20 %.

3.3. Single factor experimental analysis of ADRP extraction

3.3.1. Effect of liquid/solid ratio on ADRP yield

As illustrated in Fig. S2 (supporting information), the extraction rate of ADRP peaked at a liquid–solid ratio of 10:1 mL/g, subsequently declining as the ratio increased. This decrease can be attributed to a reduction in polysaccharides concentration within the solution due to the higher solvent volume, leading to an increased pressure difference in polysaccharides molecular diffusion (Qian et al., 2020). Further escalation of the liquid–solid ratio results in polysaccharides loss,

consequently lowering the extraction rate of polysaccharides (Guo et al., 2019). Thus, the optimal liquid–solid ratio of 10:1 mL/g was recommended.

3.3.2. Effect of ultrasonic temperature on ADRP yield

As depicted in Fig. S3 (supporting information), higher temperatures enhance mass transfer efficiency and accelerate extraction speed. The extraction rate of ADRP demonstrate an optimal temperature range. Within this range, higher temperatures increase the yield of polysaccharides extraction. Nevertheless, surpassing this temperature range decreases the polysaccharides yield, potentially caused by structural changes induced by elevated temperatures. This observation aligns with findings from previous studies on polysaccharides extraction (Huo et al., 2017). Consequently, the ideal extraction temperature for polysaccharides in this experiment was determined to be 60 °C.

3.3.3. Effect of extraction time on ADRP yield

The duration of extraction plays a pivotal role in determining the extraction rate, with longer extraction time positively impacting polysaccharides yield. Previous studies have highlighted the advantageous effects of extended extraction durations on polysaccharides production (Lin, 2014). As illustrated in Fig. S4 (supporting information), the polysaccharides extraction rate initially increased from 15 min to 25 min. However, surpassing the 25-min mark led to a decline in extraction rate. This decline could be attributed to potential hydrolysis of some polysaccharides under elevated temperatures and prolonged extraction times (Huo, 2020). Hence, the optimal extraction time was identified as 25 min.

3.3.4. Effect of ultrasonic power on ADRP yield

The extraction yield increased with the ultrasonic power augmentation in the range of 200–400 W, as illustrated in Fig. S5 (supporting information). This phenomenon can be attributed to the mechanical effect of ultra-high pressure, facilitating solvent penetration into the cell material, altering cell structure, and disrupting biological cell tissue. These changes enhance the transfer of the target extract to the solvent

Table 2

Factors and levels in BBD-RSM experimental design.

Factors	Level		
	−1	0	1
A-Ultrasonic time (min)	15	25	35
B-Ultrasonic temperature (℃)	50	60	70
C-Ultrasonic power (W)	350	400	450

Table 3

ADRP yields based on BBD-RSM design.

Run	Ultrasonic time (A, min)	Ultrasonic temperature (B, ℃)	Ultrasonic power (C, W)	Total polysaccharide yields (Y, %)
1	35	60	450	8.26
2	25	60	400	8.62
3	15	70	400	8.37
4	25	60	400	8.70
5	25	70	350	8.19
6	15	50	400	8.39
7	35	60	350	8.48
8	25	60	400	8.76
9	15	60	350	7.96
10	25	60	400	8.87
11	25	50	450	8.62
12	25	70	450	8.53
13	25	50	350	8.48
14	35	50	400	8.5
15	15	60	450	8.75
16	25	60	400	8.82
17	35	70	400	8.24

within the cell (Zhang et al., 2021). At 400 W, the extraction rate of polysaccharides peaked before declining with higher power settings. This decline is likely a result of increased stress from higher power levels and the continued mechanical effects of ultra-high pressure that further modify cellular structure, impeding the release of polysaccharides by the organism. This finding aligns with prior research indicating that ultra-high pressure can cause macromolecular denaturation (Liu et al., 2023). Therefore, an ultrasonic power of 400 W emerges as the optimal choice.

3.4. Optimization of extraction conditions by response surface method

3.4.1. Box-Behnken design

L9 (3^3) orthogonal design was adopted to further screen the experimental factors. In this work, 3 factors and 3 levels were used for extraction, as shown in Table 2. Each experiment was repeated three times.

To optimize the extraction conditions, ultrasonic time (A), ultrasonic temperature (B), and ultrasonic power (C) were varied to achieve diverse response values of polysaccharides yield. The experimental outcomes are detailed in Table 3 by employing the Box-Behnken central composite design method in Design-Expert 12.

3.4.2. Fitting the response surface model

The Design-Expert 12 software was utilized to analyze the data and determined the optimal results across various parameters. The regression equation for polysaccharides yield was derived through multiple regression analysis, conforming to the quadratic polynomial below:

$Y = 8.75 + 0.0013 \times A + 0.0825 \times B + 0.1312 \times C - 0.0600 \times AB - 0.2525 \times AC + 0.0500 \times BC - 0.2357 \times A^2 - 0.1433 \times B^2 - 0.1557 \times C^2$.

In the formula, Y is the predicted yield of ADRP, and A, B and C are the parameters of ultrasonic time, temperature and power, respectively.

The statistical significance of the data was determined through regression modeling, and the variance analysis of the response surface data is presented in Table 4.

The analysis in Table 4 reveals an impressive coefficient of determination, with $R^2 = 0.9579$, signifying the experimental model's capability to predict within the range of control variables. Utilizing p-values as a tool to assess the coefficients' significance, it was evident that smaller p-values correspond to greater coefficient significance. Notably, the primary term (C), quadratic terms (A^2, B^2, C^2), and the interaction coefficient (AC) exhibited exceptional significance ($P < 0.01$), while the linear coefficient (B) was also significant ($P < 0.05$), other term coefficients proved nonsignificant ($P > 0.05$). Furthermore, the experiment's low coefficient of variation (CV) underscores its high accuracy and reliability. By evaluating the F values for each factor, it becomes apparent that the order of influence on polysaccharides extraction rate is C > B > A, denoting ultrasonic power as the most influential, followed by ultrasonic temperature and ultrasonic time.

3.4.3. Validation of prediction model

The optimal extraction parameters included an extraction time of 21.409 min, extraction temperature of 59.903°C, extraction power of 434.912 W, and a predicted polysaccharides yield of 8.803 %. To standardize the test conditions, the independent variables were adjusted to an extraction time of 21 min, a liquid–solid ratio of 10:1 mL/g, extraction temperature of 60 °C, and extraction power of 435 W. Through three repetitions of this optimized process, the average polysaccharides extraction rate reached 8.713 %, displaying a deviation of less than 0.09 % from the predicted value. These findings affirm the model's adequacy for the extraction of ADRP, establishing the success of the response surface optimization experiment.
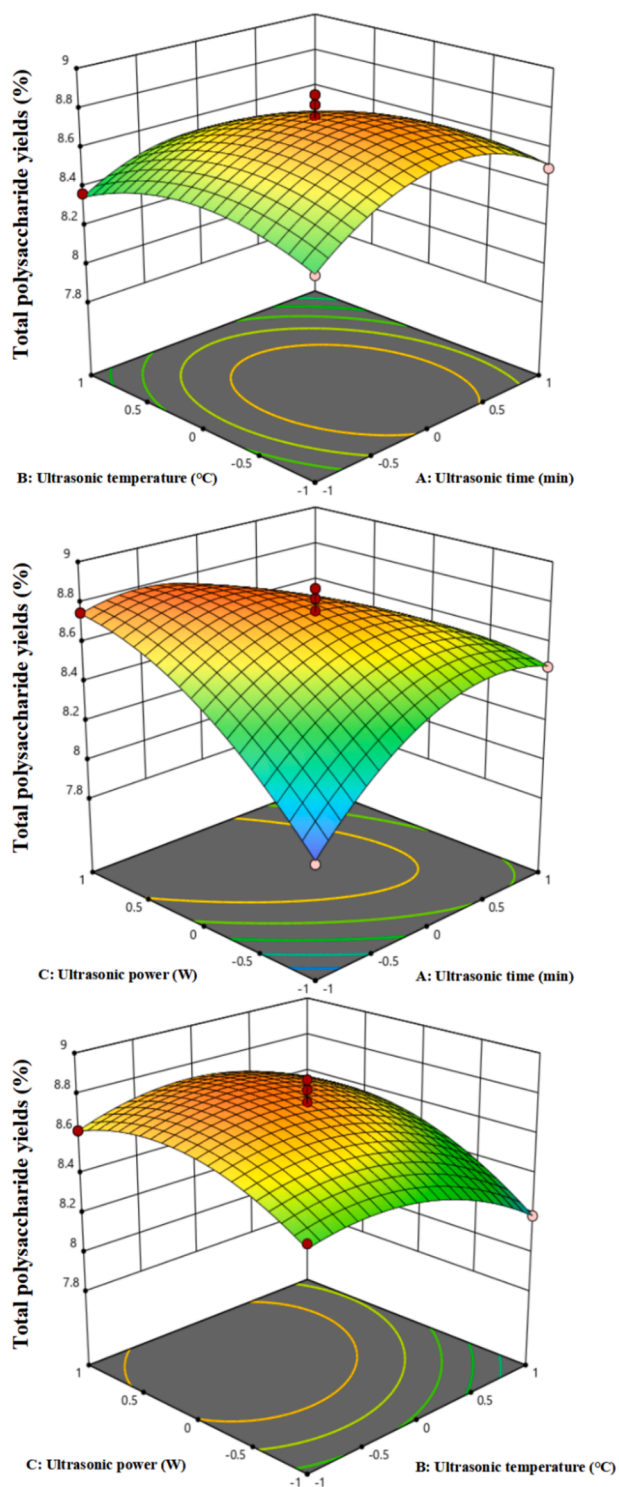
Table 4

The variance analysis table of quadratic regression model.

Variables	Sum of Squares	df	Mean Square	F-value	P-value	Significance
Model	0.9404	9	0.1045	17.71	0.0005	**
A-Ultrasonic time	0.0000	1	0.0000	0.0021	0.9646	
B-Ultrasonic temperature	0.0545	1	0.0545	9.23	0.0189	*
C-Ultrasonic power	0.1378	1	0.1378	23.36	0.0019	**
AB	0.0144	1	0.0144	2.44	0.1622	
AC	0.2550	1	0.2550	42.23	0.0003	**
BC	0.0100	1	0.0100	1.70	0.2341	
A^2	0.2340	1	0.2340	39.67	0.0004	**
B^2	0.0864	1	0.0864	14.65	0.0065	**
C^2	0.1021	1	0.1021	17.31	0.0042	**
Residual	0.0413	7	0.0059			
Lack of fit	0.0026	3	0.0009	0.0887	0.9625	#
Error	0.0387	4	0.0097			
R^2	0.9579					
CV %	0.9034					
Adj R^2	0.9039					

Note: * significant influence ($0.01 < P < 0.05$), ** extremely significant influence ($P < 0.01$), # insignificant influence.

Fig. 2. 3D response surface diagram of the two independent variables interdependency: ultrasonic time and ultrasonic temperature (a), ultrasonic time and ultrasonic power (b) and ultrasonic temperature and ultrasonic power (c).

3.4.4. 3D response surface

Design Expert 12 software was utilized to create response surface diagrams and assess various influential factors along with their interactions. The 3D response surface diagram and two-dimensional contour map depict the interdependency of the two independent variables, showcasing the effects on response variables. Specifically, the 3D diagram illustrates how independent variables interact with response variables, while the contour map demonstrates the significance of these

Table 5
Comparison of ADRP yields from different extraction methods.

Method	Temperature/Time	Extraction rate	Data source
Hot water extraction	Boiling water/2h	6.57 %	This study
Cold water extraction	25 °C/24 h	4.05 %	[39]
Hot water extraction	80 °C/3h	2.72 %	[40]
Ultrasound-assisted DES	60 °C/21 min	8.71 %	This study

interactions. The circular shape in the contour map suggests negligible interaction between variables, whereas an elliptical contour indicates substantial interaction. Fig. 2 and Fig. S6 illustrates the impact of different factor interactions on the extraction rate of ADRP. In cases of interaction between independent variables, an elliptical contour is observed.

The results in the Fig. 2 revealed that the yield of polysaccharides extraction rises with increasing ultrasonic time, while ultrasonic temperature follows a pattern of initial increase and subsequent decrease. For the approximate circular contour map of ultrasonic time and temperature, no significant interaction effect on the polysaccharides yield is observed, which is supported by the analysis of variance (AB) where P values above 0.05 confirm this finding. On the other hand, when the ultrasonic temperature (B) was set at 0, Fig. S6 demonstrates the influence of ultrasonic time (A) and power (C) on the extraction rate. The data in Fig. 2 indicates a trend where the polysaccharide extraction initially increases and then decreases with rising ultrasonic time and power. The elliptical contour diagram clearly illustrates a highly significant interaction between ultrasonic time and power, corroborated by a P value below 0.01 in the analysis of variance (AC). In summary, with a fixed ultrasound time, the impact of ultrasound power on the ADRP extraction rate surpasses that of ultrasound time, while the interrelationship between ultrasound power and ultrasound temperature shows minimal significance. Consequently, during ADRP extraction, the hierarchy of influence on ADRP yield is as follows: ultrasound power > ultrasound time > ultrasound temperature.

3.5. Comparison of different extraction processes

Table 5 presents the yields of ADRP obtained from various extraction methods. The yield of ADRP is influenced by factors such as the plant's origin, growth stage, harvest timing, processing techniques, and storage methods, resulting in notable variations in ADRP content across different batches. This study, along with previous research references, indicates that traditional water extraction methods are time-consuming and yield-poor. In contrast, the ultrasound-assisted DES extraction method developed in our research achieves an ADRP yield of 8.71 % with just 60 °C, 21 min, and 435 W low ultrasound power, effectively mitigating time and energy consumption concerns while enhancing extraction efficiency.

The interactions in DES primarily involve hydrogen bonding, electrostatic interactions, and Van der Waals forces, collectively shaping the distinctive physicochemical properties of DES (Yahaya et al., 2024). The extraction, separation, and purification of polysaccharides rely on their unique structural characteristics. The structural complexity and diversity of polysaccharides sourced from natural materials pose challenges. Nevertheless, polysaccharides are fundamentally hydrophilic macromolecules. Their extraction methods differ from small molecules, with highly polar solvents proving more effective. DES typically exhibit a higher abundance of hydrogen bonds compared to other solvents, which enhances the solubility of polysaccharides and facilitates selective extraction processes. Additionally, the versatility of DES renders it compatible with polysaccharides of varying chemical compositions.
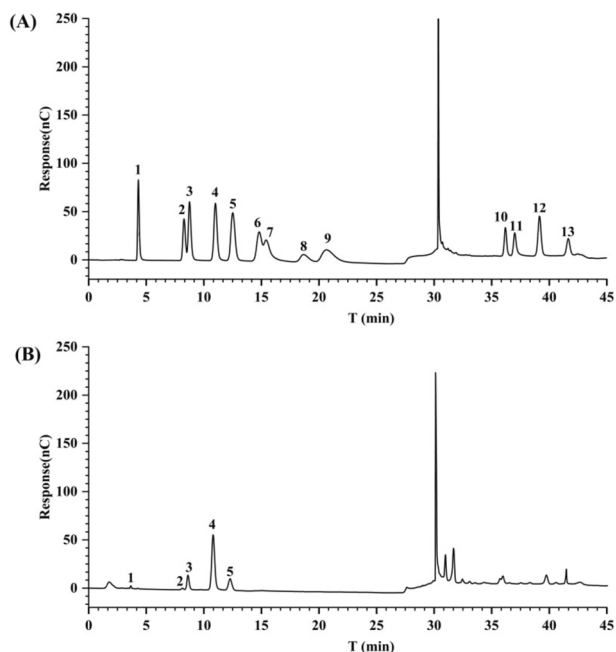
Fig. 3. Monosaccharide composition chromatogram: Reference sample profile (A) and sample profile (B). Notes: 1:fucose, 2: rhamnose, 3: arabinose, 4: galactose, 5: glucose.
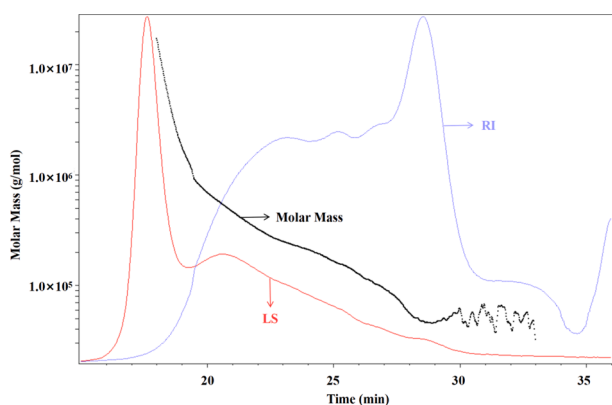

Fig. 4. Polysaccharides molecular weight distribution chart.

3.6. Identification of polysaccharides structure

3.6.1. FT-IR spectroscopy Scan

In the FT-IR spectrum (Fig. S7, supporting information), the polysaccharides powder exhibited a range of 4000–400 cm^{-1}, with distinct absorption bands identified. The broad band observed at 3228 cm^{-1} corresponds to the O-H stretching vibration, characteristic of polysaccharides, while the signal at 2925 cm^{-1} indicates C-H stretching vibration (Li et al., 2019). Additionally, peaks at 1623 cm^{-1} and 1349 cm^{-1} are attributed to the carbonyl C = O and carbonyl C-O stretching vibrations in uronic acids (Seedevi et al., 2018). The absorption band within 1000–500 cm^{-1} is primarily induced by the angular and bending vibrations of alcohols containing hydroxyl and benzene rings (Yi et al., 2022). Moreover, the peaks at 864 cm^{-1} and 1078 cm^{-1} signify the α-configuration and α-1,6-linkage (Ming et al., 2014), respectively. These findings establish that the ADRP is a heteropolysaccharide containing uronic acid (Lin et al., 2017).

3.6.2. Monosaccharide composition

After hydrolyzing the polysaccharides acid, the monosaccharide composition was analyzed by liquid chromatography (Fig. 3). The analysis disclosed that the ADRP is mainly composed of fucose, rhamnose, arabinose, galactose, and glucose, with molar ratios of 0.47:1.99:17.61:64.76:15.17.

3.6.3. Molecular weight

According to the Mark-Houwink Equation, the molecular weights of each component were determined. The number-average molecular weight was 97.422 kDa, while the weight-average molecular weight was measured at 245.678 kDa. Fig. 4 illustrates the absolute molecular weight analysis chart. In the chart, the red line represents the multiangle laser light scattering signal (LS) measured in volts (V), indicating a direct relationship between the intensity of scattered light and the molecular size and weight of the substance. The blue line shows the differential signal (RI) in Refractive Index Units (RIU), with the response value affected by changes in the effluent's refractive index post-column, reflecting the type, concentration, and molecular weight of the substance. Lastly, the black line depicts the molecular weight calculated from these combined signals.

3.7. Antioxidant activity of polysaccharides in vitro

Plant secondary metabolites and their derivatives are valuable sources for developing new natural antioxidants. Research has indicated that ADR extract exhibits significant abilities in scavenging O^{2-} and –OH radicals, highlighting its notable antioxidant properties (Zhu et al., 2014). Various studies have demonstrated that the bioactive compounds found in plant polysaccharides possess diverse biological activities, including anti-cancer, anti-viral, and antioxidant effects (Huang et al., 2017). Scholars employed 17 different DES for extracting crude polysaccharides from *camellia oleata*, leading to the discovery of evident antioxidant properties associated with these polysaccharides (Chen and Huang, 2018; Ling and Huang, 2018). In this research, the DPPH, ABTS
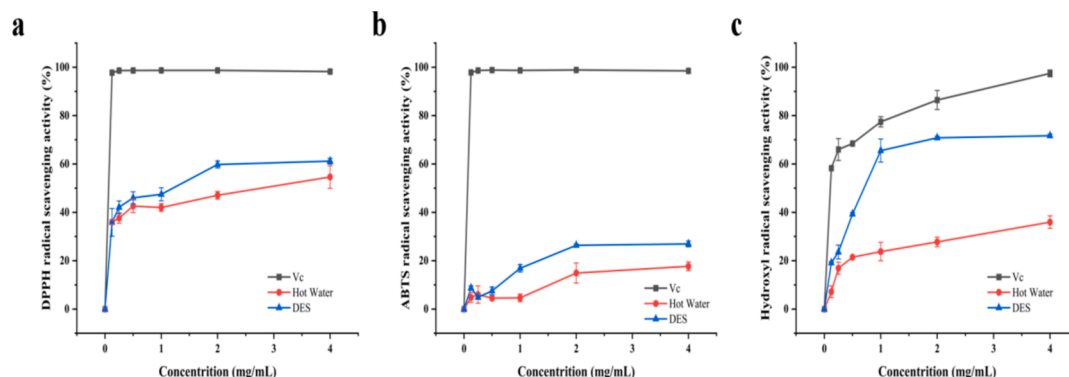

Fig. 5. Comparison of radical scavenging activity in different extraction solutions: DPPH (a), ABTS (b) and Hydroxyl (c).
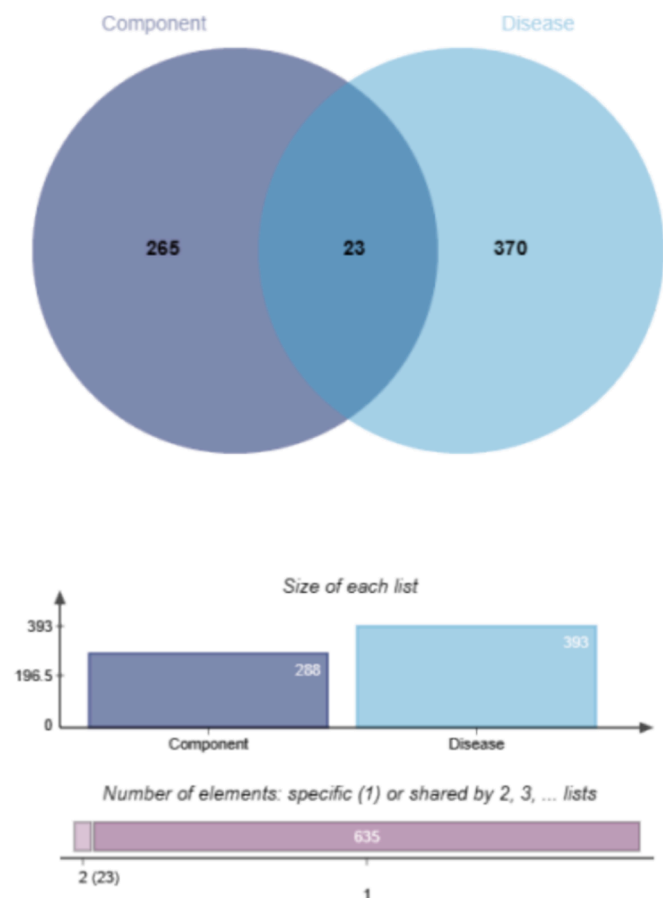
Fig. 6. Intersection Target Venn Diagram of Monosaccharides and Oxidation-Related Diseases.

and Hydroxyl radical scavenging activities of the two treatment solutions were compared with VC as the control.

The scavenging ability of extracts from various solutions increased as the mass concentration of ADRP rose, as illustrated in Fig. 5. Overall, the DES extract demonstrated robust free radical scavenging capability, surpassing hot water extraction. These findings align with prior research supporting the antioxidant activity of ADRP, likely attributed to the hydroxyl group content in polysaccharides. Hence, ADRP holds promise as a potential antioxidant in functional foods or medicines.

3.8. Network pharmacology and molecular docking

Following the acquisition of a novel environmentally-friendly and efficient extraction technique for Aqueous biphasic systems with Recyclable DES, antioxidant assessments were performed on ADRP, revealing its significant antioxidant potential. Consequently, in subsequent research endeavors, we will employ the "in silico" method to preliminarily forecast the mechanisms underpinning ADRP's in vivo antioxidant effects. Initially, in vivo targets of ADRP and Oxidation-Related Diseases were predicted by utilizing various, followed by intersecting these targets to pinpoint the specific functional targets of ADRP in vivo. The active targets were subjected to protein–protein interaction (PPI), Gene Ontology (GO), and Kyoto Encyclopedia of Genes and Genomes (KEGG) enrichment analyses to forecast their functional pathways. Lastly, molecular docking would be utilized to demonstrate the strong binding affinity between the monosaccharides present in ADRP and the identified active targets.

3.8.1. Target prediction

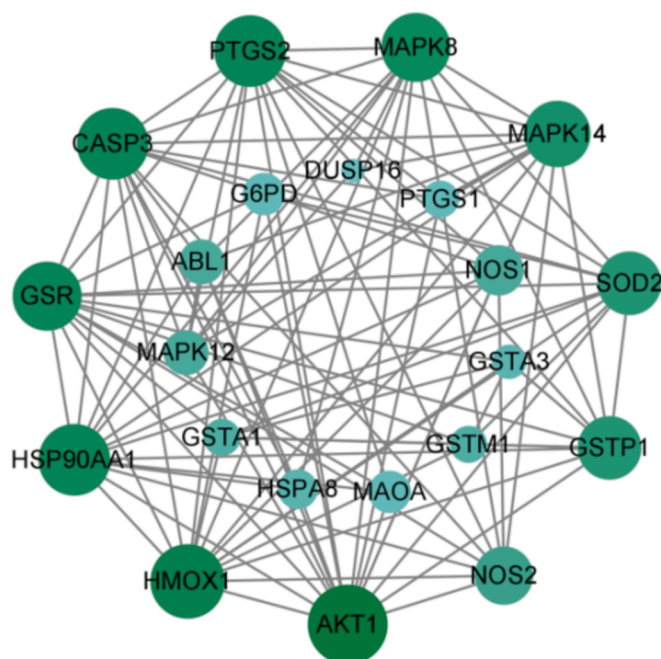The study predicted interactions between five monosaccharides and

Fig. 7. The PPI analysis of the intersection targets.

288 target sites: fucose targeted 240 sites, rhamnose 269, arabinose 243, galactose 272, and glucose 259. Additionally, the analysis identified 393 disease-related genes. Interestingly, 23 target sites were found to be shared between the monosaccharides and disease-related genes, as depicted in Fig. 6.

3.8.2. Enrichment analysis

After the analysis, predictions were made for 157 GO entries linked to the 23 common targets. These entries comprised of BP category (108), CC category (16) and MF category (33). Fig.S8 (supporting information) provides a visual representation of the top ten entries in each category, ordered by gene count.

Predictive analysis indicates that ADRP primarily partake in biological pathways such as response to oxidative stress, cellular response to chemical stress, and reactive oxygen species metabolic processes in vivo. The functional localization mainly occurs in the ficolin-1-rich granule lumen, caveolae, plasma membrane rafts, secretory granule lumen, cytoplasmic vesicle lumen, vesicle lumen, membrane rafts, etc., exerting antioxidant, glutathione transferase, peroxidase, NADP binding, heme binding, oxidoreductase activities, acting on peroxide as an acceptor, transferase activities transferring alkyl or aryl (other than methyl) groups, tetrapyrrole binding, oxidoreductase activities acting on paired donors, with incorporation or reduction of molecular oxygen, and MAP kinase activity.

A total of 88 KEGG pathways were predicted for the 23 intersecting target genes. The top ten pathways by gene count include Pathways in cancer, Metabolic pathways, etc. For detailed results, please refer to Fig. S9 (supporting information). Predicting PPI for the 23 intersection targets resulted in 22 nodes, as shown in Fig. 7, where larger nodes indicate higher degree values.

3.8.3. Molecular docking

Molecular docking of small molecules and proteins is a computational biology method used to study how small molecule compounds interact with proteins. In drug development, this method is widely used to design new drugs or optimize the structures of existing drugs. The AutoDock Vina (v1.1.2) software was utilized to conduct full-atom molecular docking analysis for the calculation of binding energies. Molecular docking analysis was conducted between the genes of the 22

−4.4	−4.9	−4.8	−4.4	−4.7	−5.2	−4.6	−4.4	−5.1	−5.1	−5.3	−5.0	−4.9	−5.1	−5.2	−5.1	−5.6	−5.4	−5.6	−5.9	−5.9	−6.0	Fuc
−4.6	−4.4	−4.7	−5.5	−4.9	−4.6	−5.2	−5.1	−4.8	−5.0	−5.5	−5.2	−5.4	−5.4	−5.4	−5.9	−5.3	−6.1	−5.9	−6.1	−6.5	−6.3	Ara
−4.5	−4.7	−4.7	−4.3	−4.9	−5.1	−5.2	−5.3	−5.1	−5.5	−5.0	−5.2	−5.6	−5.6	−5.5	−5.2	−6.0	−6.1	−5.8	−6.3	−6.2	−6.3	Gal
−4.7	−4.9	−5.2	−5.2	−5.0	−4.9	−5.2	−5.4	−5.5	−5.2	−5.1	−5.7	−5.5	−5.5	−5.7	−5.6	−6.0	−5.6	−6.2	−6.5	−6.4	−6.4	Rha
NOS2	AKT1	CASP3	NOS1	SOD2	GSTP1	MAPK12	GSTM1	MAOA	HMOX1	HSP90AA1	MAPK14	G6PD	DUSP16	MAPK8	GSTA3	PTGS1	PTGS2	ABL1	GSR	GSTA1	HSPA8	

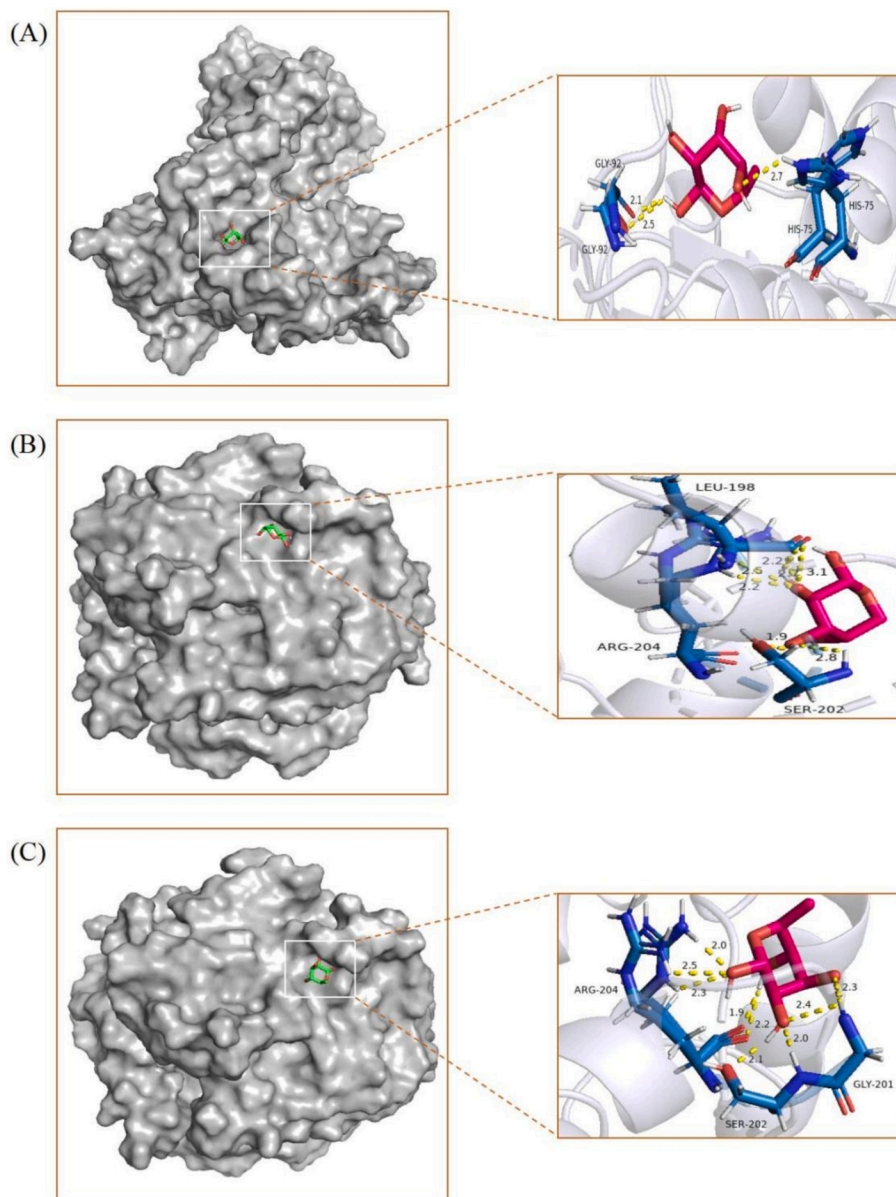**Fig. 8.** The Molecular docking binding energy of monosaccharides and proteins.

Fig. 9. Molecular docking visualization results: (A) Rha-GSR, (B) Ara-GSTA1 and (C) Rha-GSTA1.

nodes and four monosaccharides (excluding glucose), and the binding energy results are presented in Fig. 8. A trend towards red coloration corresponds to lower binding energy values, suggestive of increased binding stability.

Three sets of molecules exhibiting lower binding energies were chosen for visualization. Please refer to Fig. 9 for visualization details.

Glutathione reductase (GSR) plays a crucial role in cellular redox regulation by catalyzing the conversion of oxidized Glutathione (GSH) to its reduced form. This enzymatic process is essential for maintaining the redox balance within cells and ensuring the proper functioning of GSH. GSR serves as a key protein in the restoration and maintenance of GSH activity. GSH is ubiquitously present in the body as an antioxidant, serving as a vital non-protein protector against oxidative stress. It safeguards mitochondrial membranes from oxidative harm and contributes significantly to cytokine production and immune regulation (Lana et al., 2024). GSTA1, a member of the GST-α class, plays a critical role in neutralizing exogenous substances (including heavy metals, pesticides, organic solvents, etc.) that trigger the generation of free radicals in the body. It plays a vital role in cellular detoxification and the removal of diverse physiological compounds and xenobiotics (Grussy

et al., 2023). Hence, the robust interaction among Rha-GSR, Ara-GSTA1, and Rha-GSTA1 could represent a pivotal mechanism by which ADRP exerts antioxidative effects within the body and safeguards human health.

4. Conclusions

In this study, the optimal eutectic solvent system for extracting ADRP was selected and the experimental design was optimized by ultrasonic-assisted response surface. The results showed that the maximum extraction rate of ADRP could reach 8.713 % under the optimal extraction conditions, which was approximate to the theoretical predicted value with small error, indicating that the model was reasonable and reliable. Compared with the traditional hot water extraction method, the extraction rate of PDRP was increased by 1.33 times. In terms of extraction time, hot water extraction requires boiling water extraction for 2 h, while deep eutectic solvent system only needs 21 min to complete the extraction operation, which solves the shortage of hot water extraction time and energy, and brings a higher extraction rate, which further proves that ultrasonic assisted DES extraction method is suitable for the extraction of ADRP.

The diverse pharmacological activities and significant impacts of polysaccharides render research on these compounds with considerable medicinal value and medical importance, rendering it a prominent topic both nationally and globally. This study utilized energy-efficient and environmentally-friendly green deep eutectic solvents in conjunction with optimal extraction conditions. The experimental protocols were straightforward, resulting in a substantial polysaccharides yield, highlighting the benefits of employing DES for polysaccharides extraction. Furthermore, the research delved into the structure, antioxidant properties, and potential mechanisms of action of ADRP, laying a scientific and logical experimental foundation for the further development and application of ADRP.

CRediT authorship contribution statement

Qian Li: Writing – review & editing, Writing – original draft, Resources, Project administration, Investigation, Funding acquisition, Formal analysis, Conceptualization. **Ting Wang:** Software, Methodology, Investigation, Formal analysis, Data curation. **Chenyue Wang:** Writing – review & editing, Validation, Software, Formal analysis. **Xiaoqin Ding:** Writing – review & editing, Resources.

Declaration of Competing Interest

The authors declare that they have no known competing financial interests or personal relationships that could have appeared to influence the work reported in this paper.

Acknowledgements

Appendix A. Supplementary data

Supplementary data to this article can be found online at https://doi.org/10.1016/j.arabjc.2024.106044.

References

Chen, H.L., Huang, G., 2018. The antiviral activity of polysaccharides and their derivatives. Int. J. Biol. Macromol. 115, 77–82.

Chen, X., Wei, Z.Q., Zhu, L., et al., 2018. Efficient Approach for the Extraction and Identification of Red Pigment from *Zanthoxylum bungeanum* Maxim and Its Antioxidant Activity. Molecules 32, 1109.

Commission National Pharmacopoeia, 2020. Pharmacopoeia of the People's Republic of China. Medical Science and Technology Press, China.

Grussy, K., Laska, M., Moczurad, W., et al., 2023. The importance of polymorphisms in the genes encoding glutathione S-transferase isoenzymes in development of selected cancers and cardiovascular diseases. Mol. Biol. Rep. 50, 9649–9661.

Guo, L., Tan, D.C., Hui, F.Y., et al., 2019. Optimization of the Cellulase-Ultrasonic Synergistic Extraction Conditions of Polysaccharides from *Lenzites betulina*. Chem. Biodivers. 16, e1900369.

Huang, G.L., Mei, X.Y., Hu, J.C., 2017. The Antioxidant Activities of Natural Polysaccharides. Curr. Drug Targets. 18, 1296–1300.

Huo, D., 2020. Purification, Structure Characterization, Sulfated Modification and Activities of Water-soluble Polysaccharides from *Polygonatum ordoratum (Mill.),* Druce [D]. South China University of Technology.

Huo, Z.Q., Xu, W.Q., Liu, Y.J., 2017. Response surface methodology (RSM) was used to optimize the extraction process of polysaccharides from White Mushroom. Sci. Technol. Food Ind. 38, 5.

Lana, J.V., Rios, A., Takeyama, R., et al., 2024. Nebulized Glutathione as a Key Antioxidant for the Treatment of Oxidative Stress in Neurodegenerative Conditions. Nutrients 16 (15), 476.

Li, H., Gong, X.Q., Wang, Z.C., et al., 2019. Multiple fingerprint profile and chemometrics analysis of polysaccharides from *Sarcandra glabra*. Int. J. Biol. Macromol. 123, 957–967.

Lin, X.K., 2014. Studies on extraction and biological properties of polysaccharides from purple sweet potato [D]. Fujian Agriculture and Forestry University.

Lin, L., Xie, J., Liu, S., et al., 2017. Polysaccharide from *Mesona chinensis*: Extraction optimization, physicochemical characterizations and antioxidant activities. Int. J. Biol. Macromol. 99, 665–673.

Ling, C., Huang, G., 2018. Extraction, characterization and antioxidant activities of *pumpkin* polysaccharide. Int. J. Biol. Macromol. 118, 770–774.

Liu, Y.J., Li, L., Qun, H., 2023. Ultrasonic extraction and purification of scutellarin from Erigerontis Herba using deep eutectic solvent. Ultrason. Sonochem. 99, 106560.

Mareček, V., Mikyška, A., Hampel, D., et al., 2017. ABTS and DPPH methods as a tool for studying antioxidant capacity of spring barley and malt. J. Cereal. Sci. 73, 40–45.

Ming, M., Bai, A., Bo, J., et al., 2014. Characterisation of a novel water-soluble polysaccharide from *Leuconostoc citreum* SK24.002. Food Hydrocoll. 36, 265–272.

Qian, Y.W., Wei, J., Zhang, Z., et al., 2020. Optimization of Polysaccharides Extraction from Seed Melon by Response Surface Methodology and Its Hypolipidemic Effects in Vitro. Sci. Technol. Food Ind. 41, 7.

Seedevi, P., Moovendhanb, M., Sudharsan, S., et al., 2018. Isolation and Chemical characteristics of rhamnose enriched polysaccharide from *Grateloupia lithophila*. Carbohyd. Polym. 195, 486–497.

Shashidhar, G.M., Giridhar, P., Manohar, B., et al., 2015. Functional polysaccharides from medicinal mushroom *Cordyceps sinensis* as a potent food supplement: extraction, characterization and therapeutic potentials – a systematic review. Rsc Adv. 59, 16050–16066.

Sun, Y., Yang, B.Y., Wu, Y.M., et al., 2015. Structural characterization and antioxidant activities of kappa-carrageenan oligosaccharides degraded by different methods. Food Chem. 178, 311–318.

Sun, Y., He, L., Su, Z., et al., 2021. Ultrasonic-assisted Eutectic Solvent Extraction of *Glycyrrhiza* Polysaccharide. Food Res Dev 42, 84–91.

Tomas, Z., Petra, O., Maria, A.S., et al., 2018. Determination of storage (starch/glycogen) and total saccharides content in algae and Cyanobacteria by a phenol-sulfuric acid method. Bio-Protocol. 8, e2966.

Wang, Q., Li, Y., Wang, S., et al., 2023a. A review of the historical records, chemistry, pharmacology, pharmacokinetics and edibility of *Angelica dahurica*. Arab. J. Chem. 16, 104877.

Wang, J., Lian, P., Yu, Q., et al., 2017. Purification, characterization and procoagulant activity of polysaccharides from *Angelica dahurice* roots. Chem. Cent. J. 11, 1–8.

Wang, Y., Xiong, X., Huang, G., 2023b. Ultrasound-assisted extraction and analysis of maidenhairtree polysaccharides. Ultrason. Sonochem. 95, 106395.

Wang, C., Zhang, J., Wang, F., et al., 2013. Extraction of crude polysaccharides from *Gomphidius rutilus* and their antioxidant activities in vitro. Carbohyd. Polym. 94, 479–486.

Xie, J.H., Dong, C.J., Nie, S.P., et al., 2015. Extraction, chemical composition and antioxidant activity of flavonoids from *Cyclocarya paliurus* (Batal.) Iljinskaja leaves. Food Chem. 186, 97–105.

Yahaya, N., Mohamed, A.H., Sajid, M., et al., 2024. Deep eutectic solvents as sustainable extraction media for extraction of polysaccharides from natural sources: Status, challenges and prospects. Carbohyd. Polym. 338, 122199.

Yi, J.P., Li, X., Wang, S., et al., 2022. Steam explosion pretreatment of *Achyranthis bidentatae* radix: Modified polysaccharide and its antioxidant activities. Food Chem. 375, 131746.

Zhang, F., Sun, Z., Li, X., et al., 2023. Ultrasound-assisted alkaline extraction of protein from *Tenebrio molitor* larvae: Extraction kinetics, physiochemical, and functional traits. Ultrason. Sonochem. 95, 106379.

Zhang, S., Yi, W., Wang, Z., et al., 2021. Ultrahigh pressure extraction of polysaccharide from *Morinda officinalis* and effect on the polysaccharide structure. Sep. Sci. Technol. 56, 1741–1751.

Zhu, Y.X., Li, B.L., Ma, H.S., et al., 2014. Research progress of *Angelica dahurica* for extracting effective components, pharmacological action and clinical application. China Medical Herald. 11, 5.